Electrochimica Acta 231 (2017) 216–222

Contents lists available at ScienceDirect

Electrochimica Acta

journal homepage: www.elsevier.com/locate/electacta

Towards core-shell bifunctional catalyst particles for aqueous metal-air batteries: NiFe-layered double hydroxide nanoparticle coatings on γ-MnO_2 microparticles

Andreas Flegler[a], Stephan Müssig[a,b], Johannes Prieschl[a], Karl Mandel[a,b,*], Gerhard Sextl[a,b]

[a] Fraunhofer Institute for Silicate Research ISC, Neunerplatz 2, 97082, Wuerzburg, Germany
[b] Department of Chemical Technology of Materials Synthesis, University of Wuerzburg, Roentgenring 11, 97070, Wuerzburg, Germany

ARTICLE INFO

Article history:
Received 13 October 2016
Received in revised form 26 January 2017
Accepted 30 January 2017
Available online 4 February 2017

Keywords:
NiFe LDH
layered double hydroxides
metal-air batteries
OER
bifunctional catalyst

ABSTRACT

Herein, we investigated the synthesis of a bifunctional catalyst particle system for aqueous metal-air batteries. To target a system which possesses both, oxygen evolution reaction (OER) and oxygen reduction reaction (ORR) capabilities, γ-MnO_2 microparticles were combined with NiFe layered double hydroxides (LDH) to a core-shell system. NiFe-LDH can be optimized in its constituency to yield a very low onset potential (at 10 mA cm^{-2}) for the oxygen evolution reaction of only 569 mV vs. Hg/HgO. We investigated different coating processes (in-situ precipitation coating and sonochemical assisted coating) in order to create a bifunctional system of LDH shell@γ-MnO_2 core. It was found that the overall catalytic functionality of the bifunctional system strongly depends on the coating process, as this ultimately determines the surface nature and thus the behavior in ORR and OER reactions, respectively, of this core-shell system.

1. Introduction

The demand for energy storage systems for mobile and stationary applications is rapidly increasing. Currently, the most widespread energy storage system for mobile applications like notebooks or mobile phones is the lithium-ion battery (LIB) technology. However, this technology is already exploited close to its limits regarding the extractable theoretical energy density (387 Wh kg^{-1}) [1]. Therefore, due to their much higher theoretical energy densities, metal-air batteries come into focus as the battery systems of the future. For instance, the theoretical energy density of Li-O_2 (aq) is 3582 Wh kg^{-1} and for the Zn-air system, the values are still remarkably high at 1086 Wh kg^{-1} [1]. The working principle of metal-air batteries is that during discharge, oxygen is reduced to hydroxide ions. This reaction is called the oxygen reduction reaction, ORR. During charging, oxygen is formed. This reaction is called the oxygen evolution reaction, OER [1,2]. Unfortunately, one of the greatest challenges for this kind of batteries is the high overpotential by the air-cathode, i.e., at the so called gas diffusion electrode "GDE" and which occurs with both, the ORR and the OER. To reduce the overpotentials for the OER and the ORR, respectively, suitable catalysts are needed. That is why there is an ongoing search among many different classes of materials to find the best catalyst system. Examples of the most promising candidates that were reported so far include noble metals, transition metal oxides and carbon materials [2–4]. The highest catalytic activity for the OER, which is also very important for electrochemical oxidation of water, is observed for catalysts including Pt, Ru, Ir and Ni [4–6]. Detrimental to the use of these catalysts are the high costs for the noble metals and the heat treatment, necessary during synthesis [6].

Herein, we report on a system which is free of any noble metals, fast, simple and cheap to synthesize and which shows a promising potential. The key material class we focused on in our work is the class of the so called layered double hydroxides (LDH). LDHs are anionic clays with positively charged metal hydroxide layers which can be intercalated with anions such as carbonate [7]. LDH-based materials are interesting for a broad range of applications as they for instance may act as adsorbers for anions, as adsorbers for gases but also as flame-retardant agents to name but a few [8–15]. By using Ni and Fe as metal cations in the LDH structure, a very active OER catalyst can be obtained, which was reported recently [16–22].

* Corresponding author.
E-mail address: karl-sebastian.mandel@isc.fraunhofer.de (K. Mandel).

http://dx.doi.org/10.1016/j.electacta.2017.01.179
0013-4686/

Ideally, a particle with bifunctional properties is favoured, i.e., a particle system that possesses both, OER and ORR capabilities. We targeted this by a core-shell approach where we used the NiFe-LDH as shell, coated on an ORR active microparticle core. The approach to use bifunctional particles instead of mixing both catalysts has a crucial advantage when it comes to processing the materials. In a later application of the catalysts in a gas diffusion electrode it is difficult to distribute two different types of particles (with different particle size, morphology, surface chemistry etc.) homogenously in the reactive layer of the electrode. Any special inhomogeneity bears the danger to yield non-controllable fluctuations in the final catalytic performance of the system. Thus, the device design and production process is much easier if only one catalyst particle is used, which bears a bifunctional activity.

Initially, we investigated the electrochemical OER activity of NiFe-LDH particles as function of their structure/composition, which was varied by either deliberately intercalating carbonate or recrystallizing the structure upon a post-synthesis thermal treatment. From the results of these initial investigations, the best NiFe-LDH structure was selected to create a bifunctional catalyst particle by combining the OER-active NiFe-LDH with micron-sized γ-MnO_2 catalyst particles which are known to be ORR active. By evaluating different coating approaches, we found a relation between the coating mechanism and the ORR and OER potential of this bifunctional system.

2. Experimental

2.1. Chemicals

$NiCl_2{\cdot}6H_2O$ and $FeCl_3{\cdot}6H_2O$ were purchased from Sigma Aldrich, Germany at 99.999 % purity grade, NaOH pellets were obtained from VWR, Germany and Na_2CO_3 from abcr GmbH, Germany (purity: 99.5 %). The γ-MnO_2 microparticles were synthesized as described in an earlier work from us [23]. Potassium hydroxide pellets, *n*-propanol and Nafion solution (5 wt-% solution) were purchased from Sigma Aldrich, Germany. All chemicals were used as received without further purification.

2.2. Synthesis of NiFe-LDH

For the synthesis of the selected LDH system that contains nickel and iron with a molar ratio of 2:1, 0.43 g (1.8 mmol) nickel(II) chloride hexahydrate ($NiCl_2.6H_2O$) and 0.24 g (0.9 mmol) iron(III) chloride hexahydrate ($FeCl_3{\cdot}6H_2O$) were dissolved in 10 ml deionized water (*Solution I*). A *Solution IIa* was prepared by dissolving 0.24 g (6 mmol) sodium hydroxide (NaOH) in 40 ml deionized water under stirring. Optionally, 0.19 g (1.8 mmol) sodium carbonate (Na_2CO_3) was added to *Solution II* (denoted as *Solution IIb*). Subsequently, *Solution I* was added to *Solution IIa* (respectively *Solution IIb*) drop by drop with continuous stirring for 2 min. After stirring the product for another 3 min, the precipitate was washed. This was done by centrifuging the dispersion at a rotation speed of 5000 rpm for 15 min with a Z513 K, HERMLE centrifuge. Subsequently, the clear supernatant was decanted and the sedimented LDH was redispersed for 5 min in 25 ml deionized water. This procedure was repeated four times. Eventually, the product was redispersed in deionized water. The weight fraction of the solid content in the final dispersion was determined gravimetrically by drying a part of the suspension at 120 °C for at least 18 h.

To carry out recrystallization experiments, the whole procedure as described above to prepare NiFe-LDH with and without carbonate was repeated and the final product was taken and recrystallized for 114 h at 80 °C in deionized water.

2.3. Synthesis of a γ-MnO_2-core NiFe-LDH-shell composite particle system

γ-MnO_2 microparticles were coated by two different mechanisms with NiFe-LDH as follows:

2.3.1. Sonochemical assisted coating

100 mg of γ-MnO_2 microparticles were coated with 10 mg NiFe-LDH (10 wt% coating) by means of sonochemistry as follows: The γ-MnO_2 were dispersed in a NiFe-LDH suspension which contained 10 mg solid LDH. After the pH was adjusted to 8-9 with 1 M potassium hydroxide, the suspension was exposed to ultrasound for 5 minutes in total. This was done with a sonic horn (ultrasound device: Sonics & Materials VCX130) which exposed the dispersion to ultrasound pulses with a length of 2 s in burst mode every 5 s.

2.3.2. In-situ precipitation-coating

500 mg γ-MnO_2-particles were dispersed in *Solution IIa*. Subsequently, *Solution I*, containing Ni^{2+} and Fe^{3+} salts, was added drop by drop with stirring.

The samples that were received from the coating-procedures *A)* and *B)*, respectively, were treated identically afterwards as described in the following: To remove any non-deposited LDH, the reaction product was pressure-filtrated through a filter with a pore size of 0.8 μm and a pressure of ρ = 1 bar. The remaining micron sized composite core-shell particles (γ-MnO_2-core-LDH-shell) were washed and filtered again three times with 20 ml deionised water. Eventually, the product was dried until weight constancy for at least 18 h at 120 °C.

2.4. Electrochemical characterization

The catalytic activity (ORR and OER) of the particles was analysed by rotating disc electrode (RDE, pine instruments) measurements. 20 mg of catalyst particles were dispersed in 7.96 g H_2O, 2 g *n*-propanol and 40 μl Nafion solution (5 wt-% solution) by ultrasonic (Sonics & Materials VCX130) treatment for 5 min. To prepare the working electrode, 20 μl of the catalyst ink was dropped on a mirror polished glassy carbon RDE tip (diameter: 5 mm) and dried for 15 min at 35° C. All measurements were carried out in 1 M $KOH_{(aq)}$ with a glassy carbon rod as counter electrode and Hg/HgO (1 M $KOH_{(aq)}$) as reference electrode.

The ORR polarization curves were recorded in O_2 saturated 1 M $KOH_{(aq)}$ at a potential range between 0.1 V and −0.6 V vs. Hg/HgO and a scan rate of 5 mV s^{-1} at rotation rates of 100, 140, 250, 400, 900, 1600 and 2500 rpm. The ORR onset potential was calculated at a constant current density of −1 mA cm^{-2} and a rotation rate of 900 rpm. The corresponding OER curves were carried out in Ar saturated 1 M $KOH_{(aq)}$ in a potential range between 0.2 and 0.75 V vs. Hg/HgO and a scan rate of 5mV s^{-1} at a rotation rate of 900 rpm. The OER onset potential was calculated at a constant current density of 10 mA cm^{-2}.

2.5. Analytical instrumentation

The structure and morphology of the LDH particles were studied by scanning electron microscopy (SEM, Zeiss Supra 25 SEM) at 3 keV (field emission). The zeta potential of the particles as function of pH was measured with a Malvern Instruments Zeta Sizer Nano. For the zeta potential measurements, the pH was adjusted by 0.1 M NaOH and 0.1 M HCl. The crystal structure of LDH investigated using X-ray diffraction (XRD, PANanalytical 943006003002 Empyrean Series). The XRD patterns were recorded, using Cu Kα radiation (λ = 0.15406 nm) in a range

between 5 and 80 2θ with a step size of 0.00164 2θ and a count time of 60 s. The specific surface area was calculated by the Brunauer-Emmett-Teller (BET) method from the N_2 adsorption/desorption isotherms (Quantachrom Autosorb-3B). The fraction of coated NiFe-LDH on γ-MnO_2 was analysed by X-ray fluorescence spectroscopy (XRF, AXIDOS DY 1495). The distribution of NiFe-LDH on γ-MnO_2-particles was detected by scanning electron microscopy (SEM, Zeiss Ultra 55) at 5 keV (field emission) and energy dispersive X-ray spectroscopy (EDX, Ametek EDAX SiLi-detector).

3. Results and Discussion

Initially, the effects of intercalation of carbonate into the NiFe-LDH and the influence of post-treatment by temperature to enforce LDH recrystallization were investigated with respect to their influence on the catalytic activity for the oxygen evolution reaction (OER). The core-shell system was omitted at this stage and this preselection of the best NiFe-LDH structure was conducted only on their pure NiFe-LDH.

3.1. Influence of carbonate and recrystallization on the OER catalytic performance of NiFe-LDH

From co-precipitation of Ni:Fe at a ratio of 2:1 under the conditions as described in the experimental section, nano-NiFe-LDH particles are obtained – as depicted in the SEM image in Fig. 1a. The particle morphology is rather round and no platelets are visible, although the latter would be the expected form of an ideal LDH crystal. The same observation is made for the as-precipitated NiFe-LDH when carbonate is present in excess during the synthesis (Fig. 1b). The role of carbonate was investigated as it is well known from literature that carbonate preferentially intercalates between the layers of LDH and might, therefore, have a noticeable influence on the catalytic performance of the particles during the OER. After recrystallization of the sample shown in Fig. 1a at 80 °C for 4 days, it was observed that the shape of the particles changed from round to platelet-like (Fig. 1c). This observation is in accordance with findings we made earlier and discussed in more detail in a previous publication to which we refer for further explanations [24].

The specific surface area increased by a factor of about 10 from ~8 $m^2\ g^{-1}$ to ~83 $m^2\ g^{-1}$ after recrystallization. The NiFe-LDH synthesised with an excess of carbonate did not undergo any significant change in shape after recrystallization (Fig. 1d) although the surface area increase here as well, namely from about 8 $m^2\ g^{-1}$ to ~180 $m^2\ g^{-1}$.

Fig. 2 shows the X-ray diffractograms of the pure NiFe-LDH particles. The diffractograms of all samples peak around 11° and 23° 2θ, which can be related to the rhombohedral LDH structure and which indicate the (003) and (006) crystal planes in the LDH [18]. The presence of excessive carbonate during synthesis does not have any influence on the crystallinity of the as-precipitated samples. However, samples synthesized with an excess of carbonate show a better atomic order after recrystallization at 80 °C which is indicated by the occurrence of XRD peaks at around 61° and 33° 2θ. These peaks can be related to the (110) and (113) crystal planes of LDHs. Detailed discussions on the meaning of this ordering can be found in a work we have previously published [24].

As has been reported in literature, recently, [19] NiFe-LDH show an excellent OER activity. In Fig. 3 the OER polarization curves are presented and compared to a commercial platinum catalyst (Pt@C). Comparing the synthesized LDH particles, the LDH without heat treatment and without addition of carbonate ions shows the lowest OER onset potential (569 mV vs. Hg/HgO). It is very remarkable that this onset potential is over 100 mV lower than the onset potential of the commercial Pt@C catalyst benchmark. The LDH structure with intercalated carbonate has an OER onset potential which is shifted by about 32 mV towards higher potential.

As can be seen from Fig. 3, recrystallized LDH in general yields a poorer OER activity. Particularly for NiFe-LDH synthesized in presence of carbonate, recrystallization yields an OER of about 742 mV vs. Hg/HgO which is far worse than the OER onset potential of the Pt@C benchmark. Apparently, the performance of the LDH is better, if the in-between-layer sites are not fully occupied, i.e., it is

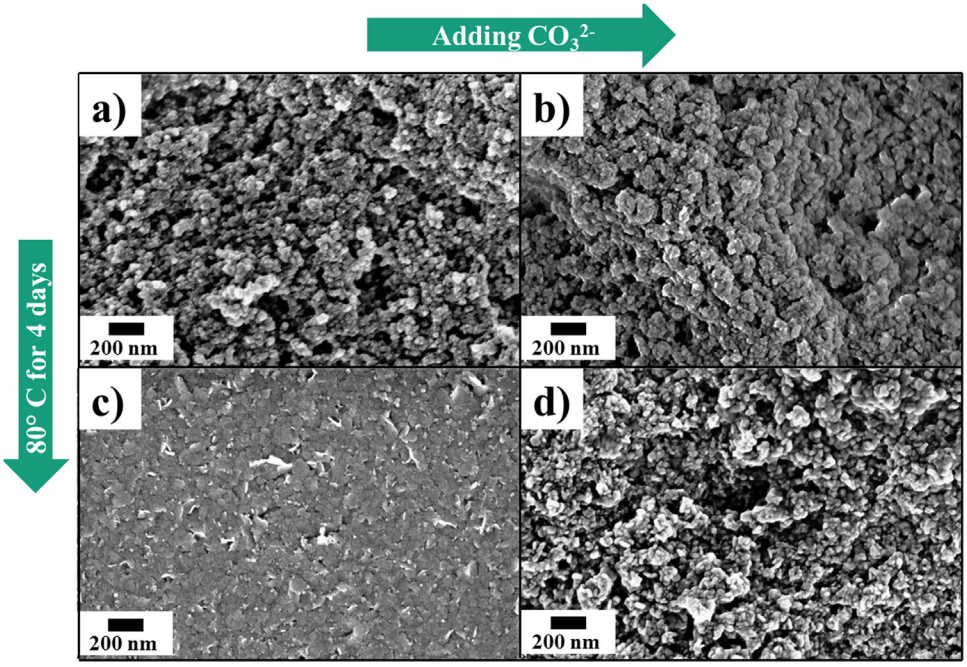

Fig. 1. SEM images of NiFe-LDH particle morphology obtained without (a) and with (b) excess carbonate presence during synthesis and after recrystallization at 80° C for 4 days: (c) is the recrystallized sample (a); (d) is the recrystallized sample (b).

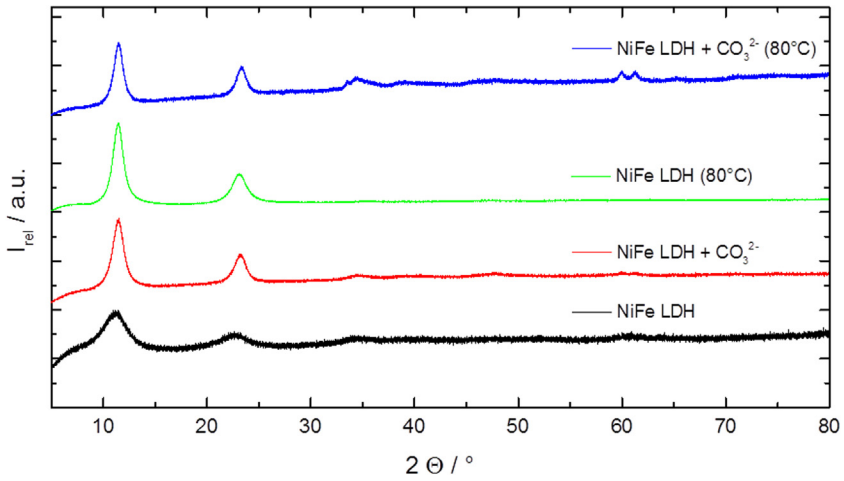

Fig. 2. X-ray diffractograms of the samples, depicted in SEM images in Fig. 1. All XRDs are normalized in intensity with respect to the (003) peak.

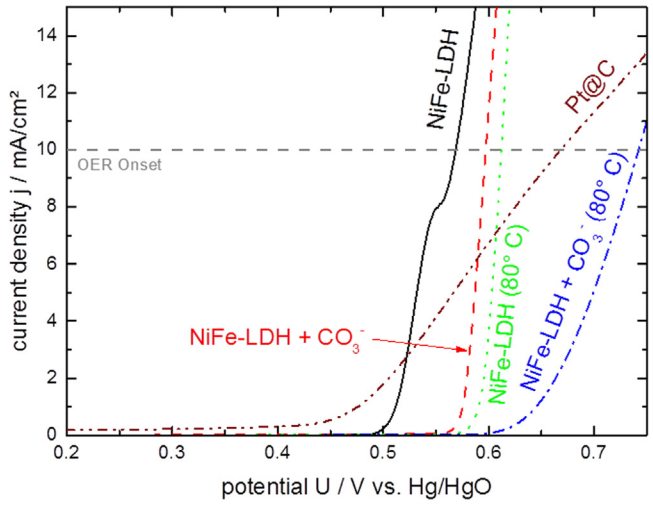

Fig. 3. OER polarization curves of the samples depicted in Fig. 1 and of a commercial Pt@C catalyst which is shown as benchmark. Measurements were performed in an Ar saturated 1 M $KOH_{(aq)}$ at a rotation rate of 900 rpm.

better to not have carbonate intercalated. This can be explained by assuming the interlayer space to be potentially catalytically active, i.e., the more spots are accessible for oxygen, the better is the performance of the catalyst. What is remarkable and counter-intuitive, however, is the finding that apparently, a higher S_{BET} does not mean a better performance. Comparing the samples synthesized without excess of carbonate before and after recrystallization in their OER performance, it can be seen that the non-recrystallized, round-shaped particles perform better than the platelets, although the latter have a tenfold higher S_{BET}. The same trend holds for the carbonate rich samples. A potential explanation is that a worse atomic ordering of Ni and Fe in the LDH structure, as it prevails in the as-precipitated samples, yields a better reactivity with oxygen, i.e., the Ni and Fe atoms are more active if they are not in a completely well-ordered state as this might put them in an energetic minimum and reduce their activity. Ultimately, this observation cannot be explained completely at this stage; however, the key finding is that as-precipitated, carbonate-free NiFe-LDH nanoparticles with a poorly ordered structure are best performing regarding the catalytic activity in an OER. Therefore, this system is selected to create the γ-MnO_2-core-NiFe-LDH-shell ORR-OER composite particles.

3.2. Coating of γ- MnO_2 with NiFe-LDH

An effective and simple method to coat nano-LDH on a microparticle core has been reported by us in the past [14]. The method works by adjusting the pH of a dispersion of the micron-sized core-particle and the LDH to be coated onto the micro-particles to a value where the surface charge of one species is positive and the surface charge of the other species is negative. Ideally, the zeta potentials of the two particle systems are as far apart as possible. Once the pH in the dispersion is set, the electrostatic attraction of the two materials is supported by exposing the dispersion to ultrasound. Due to that, the materials are forced together and are, so to say, "electrostatically welded" [14]. Fig. 4 shows the zeta potential as a function of pH for both materials, the γ-MnO_2 and the NiFe-LDH. It can be seen that below a pH value of about 10, the NiFe-LDH bears, as expected, a positive zeta potential. The isoelectric point (IEP) of the NiFe-LDH was found at a pH of about 10. γ-MnO_2 has a weakly negative surface charge above pH 4. Below pH 4 it is positively charged. The IEP is at a pH of about 4. To achieve an electrostatic attraction for the

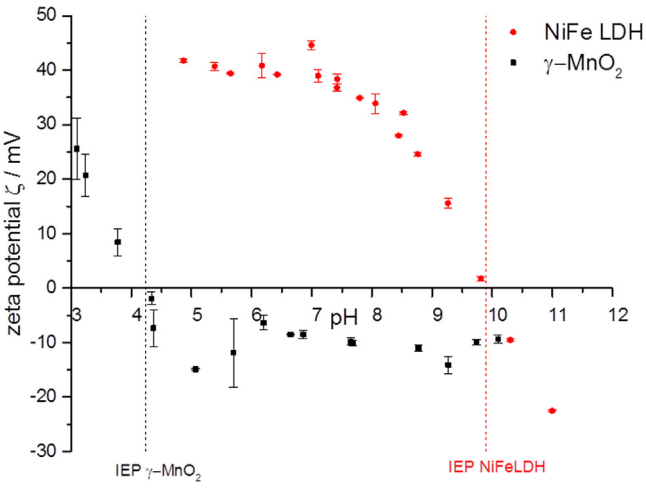

Fig. 4. Zeta potential of γ-MnO_2 and NiFe-LDH as function of pH.

coating between NiFe-LDH and γ-MnO_2, a pH of 8-9 was adjusted and the system was exposed to ultrasound (see experimental section).

Besides the sonochemical assisted coating method, in-situ precipitation was used as an alternative approach to coat NiFe-LDH onto γ-MnO_2, as described in the experimental section.

Fig. 5a shows the SEM image (inset with higher magnification) of the core-shell particles which were coated via the sonochemical assisted method. The spherical particles have the urchin-like shape of pure γ-MnO_2 particles [23]. EDX mapping results for these particles, showing the distribution of manganese and nickel, are depicted in Figures 5b and c, respectively. Nickel could be detected on all γ-MnO_2 particles. The mapping results for iron are not shown as the iron peaks overlap with the energy peaks originating from manganese. In Figure 5d, a SEM image (inset with higher magnification) of the core-shell particles which were coated via in-situ precipitation, is shown. No obvious difference to Fig. 5a can be seen. Also for this system EDX mapping was carried out (Figure 5e and f), yielding the same results as for the sonochemical-based system. It can therefore be concluded that both coating procedures, *i.e.*, the in-situ-precipitation coating and the sonochemical assisted coating, are applicable to achieve a NiFe-LDH coating on γ-MnO_2. XRD performed on the LDH-γ-MnO_2 system (not shown) did not give any hint that any form of alloy formed, thus, the particle system can be considered as γ-MnO_2-core-Ni-Fe-LDH-shell-system.

To characterize the density of the coating, zeta potential measurements as function of pH were performed with the composite system. Fig. 6 depicts the zeta potential graphs of the coated systems, and, for comparison again (from Fig. 4) the graphs for pure γ-MnO_2 and pure NiFe-LDH. It can be seen that the zeta potential versus pH curves lie somewhat in-between the two extremes of the pure systems. This is an indication for a partial, but not complete coating, which we discussed in an earlier work in more detail [25]. An increase in surface occupancy of NiFe-LDH on γ-MnO_2 results in a decrease of the influence of γ-MnO_2 on the surface charge of the composite and thus yields a zeta potential curve shift closer to that of pure NiFe-LDH. Consequently, the surface charge of samples with a higher surface loading is

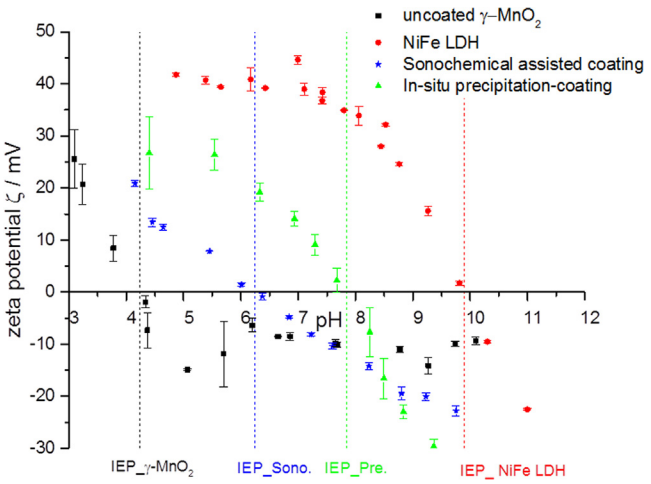

Fig. 6. Zeta potential curves of pure γ-MnO_2, pure NiFe-LDH, in-situ coating of γ-MnO_2 during precipitation of NiFe-LDH and sonochemical assisted coating.

increasingly dominated by NiFe-LDH and results in a shift of the IEP towards NiFe-LDH. Both coated samples show this shift of the IEP towards higher pH values which is, additionally to the EDX findings, an indication for a successful coating. The IEP of the sample which was coated by sonochemical assistance is shifted to a pH value of 6.2 whereas the IEP of in-situ precipitation coated γ-MnO_2 is shifted to a pH value of 7.8. Hence, at this stage, from these findings, it can be assumed that the coating of the latter sample covers more surface of γ-MnO_2 than the coating using ultrasound.

Finally, the overall catalytic performance of the core-shell composite system was determined for ORR and OER and compared to pure NiFe-LDH, pure γ-MnO_2, a mixture of the pure particles in the same ratio as present in the core-shell system, and Pt@C. The results are shown in Figure 7. As already known from literature, [16–22] the pure NiFe-LDH particles do not show any catalytic activity for the ORR (as a current density of -1 mA cm^{-2} is not

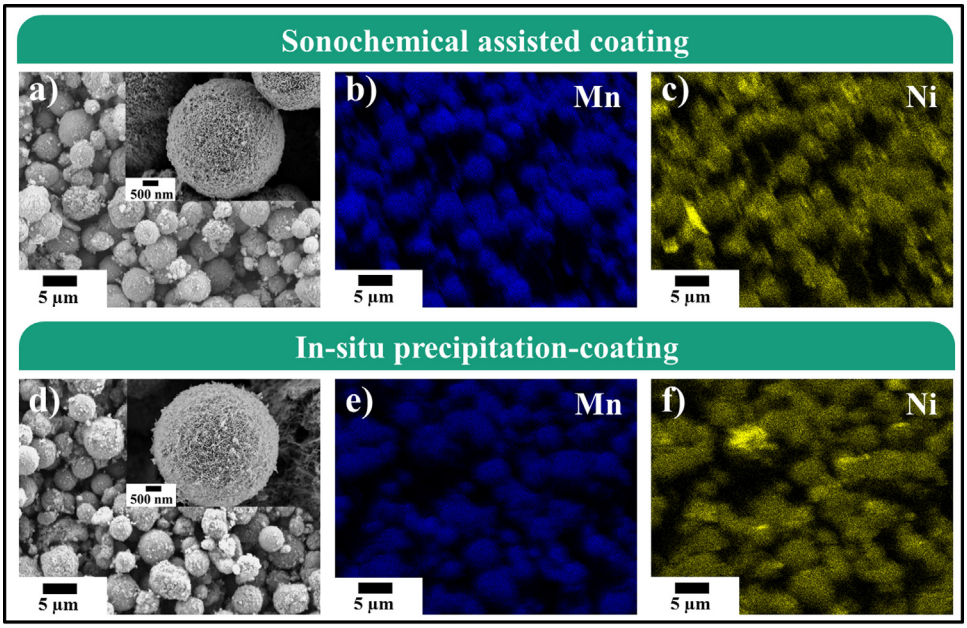

Fig. 5. SEM images (inset: higher magnification) of the core-shell particles: (a) Sonochemical assisted coating with EDX mapping for (b) manganese and for (c) nickel. (d) In-situ precipitation-coating with EDX mapping for (e) manganese and for (f) nickel.

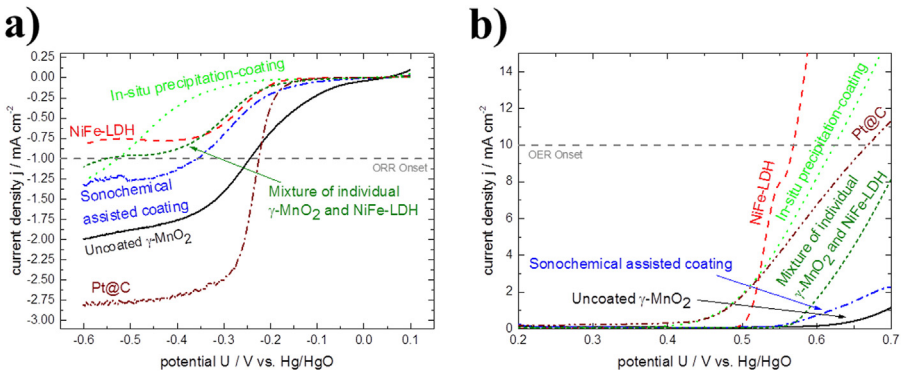

Fig. 7. RDE measurements of the pure materials, a mixture of them, bifunctional catalysts, and a commercial Pt@C catalyst. (a) ORR polarization curves in O_2-saturated KOH and (b) OER polarization curves Ar-saturated 1 M KOH at a rotation rate of 900 rpm.

reached, it is not possible to calculate an ORR onset potential). However as already shown, the OER onset potential of 569 mV (vs. Hg/HgO) is very low and thus very attractive. In contrast to that, the γ-MnO_2 catalyst has an ORR onset potential of −245 mV, which is only 19 mV lower than the ORR onset potential of Pt@C and thus very attractive as the system is free of noble-metals and, therefore, much cheaper but at almost the same performance. The OER onset potential of γ-MnO_2, however, is too high to be even detectable in the potential region relevant to be considered.

The core-shell particles are thus an attempt to combine the best of both systems.

Fig. 7 shows that the core-shell system synthesized by in-situ precipitation of NiFe-LDH onto γ-MnO_2 bears a good OER behaviour with an onset potential of 624 mV which is only 55 mV higher than for the pure NiFe-LDH catalysts. Unfortunately, the ORR activity is, although slightly better than for pure NiFe-LDH particles, relatively poor in comparison to the pure γ-MnO_2.

The core-shell particle system resulting from the sonochemical assisted coating procedure exhibits a poor OER activity in the same range as pure γ-MnO_2, but an improved ORR activity (onset potential of −356 mV) compared to pure NiFe-LDH.

To evaluate whether the co-presence of both particles leads to better catalytic properties compared to core-shell particles, the performance of a mixture of both particles in the same ratio as in case of the core-shell system was measured via the RDE method (Fig. 7). It was found that the mixed system has a similar ORR onset potential as the core-shell particle system synthesized via in-situ precipitation. However, the OER activity is much lower compared to the core-shell particle system. Thus, from these measurements, it can be stated that a mixture of the two systems does not come with an advantage. However, it should be noted that Dresp et al. [26] found that a 1:1 mixture of the ORR catalyst Fe-N-C with the OER catalyst NiFe-LDH/C leads to both, a good ORR as well as OER performance. With a 1:1 ratio, however, they used a much higher concentration of OER particles. As such a ratio could not be achieved with our core-shell systems, the performance reported cannot be directly compared to our system. The potential drawback of a "just mixed" catalyst system during processing to a final battery system was discussed in the introduction.

Taken together all findings, it can be concluded that the core-shell catalyst system synthesized by in-situ precipitation exhibits an OER/ORR catalytic behaviour more like NiFe-LDH whereas the situation is exactly vice versa for the sonochemical assisted coating procedure. XRF results revealed that the quantitative coating fraction for both coating methods is equal. In both cases, the weight fraction of the elements Ni + Fe was 6 wt-% and of MnO_2 92 wt-%. Although for both coating methods the same ratio between core and shell is achieved, the sonochemical assisted coating shows a catalytic activity more like γ-MnO_2. This might be explained by assuming that through the introduced ultrasound energy, the NiFe-LDH nanoparticles are pushed more deeply into the urchin-like structure of γ-MnO_2 in comparison to the in-situ precipitation coating. In the latter case, the NiFe-LDH particles rather grow on the outer surface of the γ-MnO_2 particles and therefore exhibit a more NiFe-LDH-like surface. It should be noted that the difference of degree of coating penetration into the γ-MnO_2 structure cannot be revealed by EDX as the X-ray information is obtained not only from the outermost surface but a certain "penetration depth"/"depth of origin of information" has to be taken into account.

Ultimately, it can be concluded that from these findings, we revealed that it is not only crucial *which* materials are combined in a core-shell system but also *how* they are combined. The core-shell formation procedure might have a severe influence on the surface character of the core-shell system which apparently dominates the overall character and thus the performance of the system in catalytic reactions. This needs to be kept in mind when creating core-shell systems.

4. Conclusion

In this work, it could be ascertained that there is an ideal NiFe-LDH constituency to yield an impressive OER activity. This is achieved by avoiding excess carbonate during the LDH synthesis and using the as-precipitated system which does not possess any well-ordered crystalline character. A bifunctional system with γ-MnO_2 core and the LDH as shell could be created by two coating procedures. Doing so, it was found that the overall catalytic functionality of the bifunctional system can be directed more towards a superior ORR or OER performance, respectively, depending on the degree of LDH coating density/penetration onto/into the γ-MnO_2 core which can be controlled by the type of coating procedure.

Thus, as the coating procedure might have a strong influence on the overall performance of such a bifunctional catalyst system, particular attention to this step should be paid in future.

Acknowledgements

The development of LDH with controlled chemistry and morphology has received funding within the framework of the project CO-PILOT from the European Union's Horizon 2020 research and innovation programme under grant agreement No 645993.

KM gratefully acknowledges the DECHEMA Max-Buchner-Forschungsstiftung for supporting him with the Max-Buchner

scholarship for research on using sonochemistry to make novel materials.

The authors sincerely thank Manfred Römer for the SEM analysis as well as the EDX mappings.

References

[1] P.G. Bruce, S.A. Freunberger, L.J. Hardwick, J.-M. Tarascon, Li-O2 and Li-S batteries with high energy storage, Nat. Mater. 11 (2012) 19–29.
[2] J.-S. Lee, S. Tai Kim, R. Cao, N.-S. Choi, M. Liu, K.T. Lee, J. Cho, Metal-Air Batteries with High Energy Density: Li-Air versus Zn-Air, Adv. Energy Mater. 1 (2011) 34–50.
[3] F. Cheng, J. Chen, Metal–air batteries: from oxygen reduction electrochemistry to cathode catalysts, Chem. Soc. Rev. 41 (2012) 2172–2792.
[4] I. Katsounaros, S. Cherevko, A.R. Zeradjanin, Karl J.J. Mayrhofer, Oxygen Electrochemistry as a Cornerstone for Sustainable Energy Conversion, Angew. Chem. Int. Ed. 53 (2014) 102–121.
[5] T. Reier, M. Oezaslan, P. Strasser, Electrocatalytic Oxygen Evolution Reaction (OER) on Ru, Ir, and Pt Catalysts: A Comparative Study of Nanoparticles and Bulk Materials, ACS Catal. 2 (2012) 1765–1772.
[6] X. Lv, Y. Zhu, H. Jiang, X. Yang, Y. Liu, Y. Su, J. Huang, Y. Yao, C. Li, Hollow mesoporous NiCo2O4 nanocages as efficient electrocatalysts for oxygen evolution reaction, Dalton Trans. 44 (2015) 4148–4154 (Cambridge, England 2003).
[7] V. Rives, M. Angeles Ulibarri, Layered double hydroxides (LDH) intercalated with metal coordination compounds and oxometalates, Coord. Chem. Rev. 181 (1999) 61–120.
[8] A.C.S. Alcântara, P. Aranda, M. Darder, E. Ruiz-Hitzky, Bionanocomposites based on alginate—zein/layered double hydroxide materials as drug delivery systems, J. Mater. Chem 20 (2010) 9495.
[9] N. Baliarsingh, K.M. Parida, G.C. Pradhan, Influence of the nature and concentration of precursor metal ions in the brucite layer of LDHs for phosphate adsorption—a review, RSC Adv. 3 (2013) 23865.
[10] S. Choi, J.H. Drese, C.W. Jones, Adsorbent materials for carbon dioxide capture from large anthropogenic point sources, ChemSusChem 2 (2009) 796–854.
[11] A. Drenkova-Tuhtan, K. Mandel, A. Paulus, C. Meyer, F. Hutter, C. Gellermann, G. Sextl, M. Franzreb, H. Steinmetz, Phosphate recovery from wastewater using engineered superparamagnetic particles modified with layered double hydroxide ion exchangers, Water Res. 47 (2013) 5670–5677.
[12] A. Drenkova-Tuhtan, M. Schneider, K. Mandel, C. Meyer, C. Gellermann, G. Sextl, H. Steinmetz, Influence of cation building blocks of metal hydroxide precipitates on their adsorption and desorption capacity for phosphate in wastewater—A screening study, Colloids Surf A 488 (2016) 145–153.
[13] Y. Gao, J. Wu, Q. Wang, C.A. Wilkie, D. O'Hare, Flame retardant polymer/layered double hydroxide nanocomposites, J. Mater. Chem. A 2 (2014) 10996.
[14] K. Mandel, A. Drenkova-Tuhtan, F. Hutter, C. Gellermann, H. Steinmetz, G. Sextl, Layered double hydroxide ion exchangers on superparamagnetic microparticles for recovery of phosphate from waste water, J. Mater. Chem. A 1 (2013) 1840–1848.
[15] Z. Matusinovic, C.A. Wilkie, Fire retardancy and morphology of layered double hydroxide nanocomposites, J. Mater. Chem. 22 (2012) 18701.
[16] G. Fan, F. Li, D.G. Evans, X. Duan, Catalytic applications of layered double hydroxides: recent advances and perspectives, Chem. Soc. Rev. 43 (2014) 7040–7066.
[17] Z. Jia, Y. Wang, T. Qi, Hierarchical Ni—Fe layered double hydroxide/MnO 2 sphere architecture as an efficient noble metal-free electrocatalyst for ethanol electro-oxidation in alkaline solution, RSC Adv. 5 (2015) 83314–83319.
[18] D. Kubo, K. Tadanaga, A. Hayashi, M. Tatsumisago, Multifunctional inorganic electrode materials for high-performance rechargeable metal—air batteries, J. Mater. Chem. A 1 (2013) 6804.
[19] Y. Li, M. Gong, Y. Liang, J. Feng, J.-E. Kim, H. Wang, G. Hong, B. Zhang, H. Dai, Advanced zinc-air batteries based on high-performance hybrid electrocatalysts, Nat. Commun. 4 (2013) 1805.
[20] X. Long, Z. Wang, S. Xiao, Y. An, S. Yang, Transition metal based layered double hydroxides tailored for energy conversion and storage, Mater. Today 19 (2016) 213–226.
[21] J. Wang, L. Wang, X. Chen, Y. Lu, W. Yang, Chemical power source based on layered double hydroxides, J. Solid State Electrochem. 19 (2015) 1933–1948.
[22] Y. Xu, Y. Hao, G. Zhang, Z. Lu, S. Han, Y. Li, X. Sun, Room-temperature synthetic NiFe layered double hydroxide with different anions intercalation as an excellent oxygen evolution catalyst, RSC Adv. 5 (2015) 55131–55135.
[23] A. Flegler, S. Hartmann, H. Weinrich, M. Kapuschinski, J. Settelein, H. Lorrmann, G. Sextl, Manganese Oxide Coated Carbon Materials as Hybrid Catalysts for the Application in Primary Aqueous Metal-Air Batteries, C 2 (2016) 4.
[24] A. Flegler, M. Schneider, J. Prieschl, R. Stevens, T. Vinnay, K. Mandel, Continuous flow synthesis and cleaning of nano layered double hydroxides and the potential of the route to adjust round or platelet nanoparticle morphology, RSC Adv. 6 (2016) 57236–57244.
[25] K. Mandel, M. Strasser, T. Granath, S. Dembski, G. Sextl, Surfactant free superparamagnetic iron oxide nanoparticles for stable ferrofluids in physiological solutions, Chem. Commun. (Cambridge England) 51 (2015) 2863–2866.
[26] S. Dresp, F. Luo, R. Schmack, S. Kühl, M. Gliech, P. Strasser, An efficient bifunctional two-component catalyst for oxygen reduction and oxygen evolution in reversible fuel cells, electrolyzers and rechargeable air electrodes, Energy Environ. Sci. 9 (2016) 2020–2024.